Biotechnology and Bioprocess Engineering 22: 76-82 (2017)
DOI 10.1007/s12257-016-0511-z

RESEARCH PAPER

# Preparation and Preliminary Evaluation of Macroporous Magnetic Agarose Particles for Bioseparation

**Jia-Li Gu, Hong-Fei Tong, and Lai-Yu Sun**

Received: 23 September 2016 / Revised: 8 November 2016 / Accepted: 7 December 2016


**Abstract** Macroporous magnetic agarose particles (MMAPs) were prepared with calcium carbonate as the porogent by the water-in-oil suspension thermal regeneration method. MMAPs with good sphericity and appropriate particle size were obtained. The physical properties of the beads were determined and it was found that the water content (92.1%), porosity (94.4%) and mean pore diameter (120.1 nm) of the MMAPs were higher than those for the normal magnetic particles, indicating successful generation of macropores after calcium carbonate addition. Compared with normal magnetic particles, the mass transfer of biomolecules in MMAPs was remarkably enhanced. Finally, MMAPs were modified with 5-amino-benzimidazol (ABI) ligand and the adsorption capacity of IgG reached 153 mg/mL, higher than that of the normal magnetic particles (126 mg/mL). Moreover, adsorption behavior of MMAPs to IgG was little changed after twenty-five recycled use. Hence, MMAPs prepared herein showed great potential for bioseparation.

**Keywords:** magnetic particle, agarose, macroporous, calcium carbonate, bioseparation

## 1. Introduction

Magnetic separation technology based on the functional magnetic particles (MPs) is of particular interest in the field of bioseparation due to its great advantages [1-3]. Compared with conventional separation technologies, such as chromatography and extraction, magnetic separation is relatively simple, economic and efficient, and no special equipment required. It could allow the capture of biomolecules from unclarified feedstock without prior removal of articulates. Moreover, MPs could be separated easily from the aqueous solution in less than 20s [4].

The performance of magnetic separation process is determined by the properties of MPs, and much effort has been made to design appropriate MPs [1,5,6]. Among which, magnetic agarose particles are the most widely used ones, due to their physical and chemical stability, easy surface modification and biocompatibility [7,8]. However, these particles usually possessed small pores with a diameter comparable to the size of a diffusing macromolecule, intraparticle diffusion of macromolecules was hindered by the steric and electrostatic interactions between them and the media [9,10]. Thus the diffusivities of biomolecules in porous media are generally two to three magnitudes lower than those in free solution, and slow intraparticle mass transfer is the rate-controlling step for the adsorption process [11]. As a result, tailing the pore size of porous media to improve the mass transfer and absorption efficiency is important.

Fabrication of macroporous media with the aid of porogenic reagent has been proven to be an efficient strategy. To date, macroporous/superporous agarose particles have been successfully used in the chromatography separation process as the stationary phase [11,12]. However, to our knowledge, there were few reports about the preparation and application of magnetic macroporous agarose particles (MMAPs).

In the present work, MMAPs were synthesized with the method of water-in-oil suspension thermal regeneration

Jia-Li Gu*, Lai-Yu, Sun
College of Life Sciences, Huzhou University, Huzhou 313-000, China
Tel: +86-572-8795-1982; Fax: +86-572-8795-1982
E-mail: gujiali@zjhu.edu.cn

Hong-Fei Tong
Key Laboratory of Biomass Chemical Engineering of Ministry of Education, College of Chemical and Biological Engineering, Zhejiang University, Hangzhou 310-027, China

using calcium carbonate as porogenic reagent. The physical properties including wet density, size distribution, water content, and porosity, and the mass transfer characteristics of MMAPs were studied and compared with normal particles. Finally, MMAPs were modified with 5-amino-benzimidazol (ABI) ligand and the protein absorption performances were investigated to evaluate the potential of MMAPs prepared for bioseparation.

## 2. Materials and Methods

### 2.1. Materials

Agarose, nano-$Fe_3O_4$ (average diameter 20 nm) and calcium carbonate (average diameter 0.8 μm) were purchased from Aladdin Co., Ltd. (Shanghai, China). GS-1 vacuum-pump oil was purchased from Sifang special oil factory (Beijing, China). Bovine serum γ-globulin (IgG purity >96%) was purchased from Tokyo Kasei Kogyo Co., Ltd. (Tokyo, Japan). Bovine serum albumin (BSA, 67 kDa) and lysozyme (14.9 kDa) were purchased from Sigma (Milwaukee, WI, USA). Other reagents were of analytical reagent grade from the local sources.

### 2.2. Preparation of MMAPs and normal magnetic agarose particles (MAPs)

The MMAPs were prepared through water-in-oil suspension thermal regeneration method. Briefly, vacuum-pump oil containing 3 wt% of emulsifiers, which were consisted of span-80 and tween-80 (w/w = 2:1), were added into a 500 mL flask. The oil phase was stirred at 800 rpm and heated to 70°C in a water bath. And then, 2.0 g agarose powder, 0.48 g sodium chloride, 0.5 g $Fe_3O_4$ and 0.5 g calcium carbonate were added into 50 mL deionized water and heated to obtain 4% (w/v) agarose solution. The agarose solution (50 mL) was then dispersed in the oil phase (300 mL) with continuous stirring at 70°C for 30 min. Thereafter, the reaction system was cooled quickly with an ice-cold water bathing. The particles were collected and washed successively with ethanol and deionized water. The particles were then mixed with 3% (v/v) epichlorohydrin and 1 mol/L NaOH by 150 rpm agitation at 30°C for 6 h to complete the cross-link reaction. The cross-linked particles were washed with deionized water thoroughly, and 0.1 M HCl was added slowly to remove calcium carbonate. The suspension was shaken in an incubator until no bubbles were observed. Finally, the particles were washed with deionized water, and stored in 20% ethanol.

Normal magnetic agarose particles (MAPs) were prepared using the same conditions without calcium carbonate addition.

### 2.3. Morphology and physical properties of MMAPs

The morphology of MMAPs was observed with a Nikon E200 microscope (Nikon Jiangnan Optical Instruments, Nanjing, China). The fine shapes and porous structures were examined by a Hitachi S-4800 scanning electron microscope (SEM) (Hitachi Instruments, Tokyo, Japan). In order to keep the real morphology of porous structure without the false impressions of SEM pictures for hydrogels, the particles were treated gradually with the solvent displacement from water to 100% ethanol, and then frozen and dried in a critical point drying apparatus (Quorum K850, United Kingdom) before SEM examination. The particle size distribution and mean particle diameter ($d$) was determined with a laser particle size analyzer (Mastersizer 2000, Malvern Instruments, Worcestershire, United Kingdom).

Other physical properties were measured according to previous reports [13]. The wet density ($\rho_p$, g/mL of wet gel) was determined by water replacement in a 5 mL gravity bottle. The value of water content ($\omega$, %) was obtained by dehydration at 120°C to a constant weight. Presuming all the pores in the particles were full of water, porosity $P$ (%) representing pore volume per volume wet particles and pore volume $V_p$ (mL/g dry beads) representing pore volume per gram dried particles are calculated as follows,

$$P=\frac{\rho_p\cdot\omega}{\rho_w}\times 100\% \tag{1}$$

$$V_p=\frac{\omega}{(1-\omega)\cdot\rho_w}\times 100\% \tag{2}$$

where $\rho_w$ means the density of water,

The specific surface area ($S$, $m^2$/mL) was determined by the adsorption of methylene blue solution as follows,

$$S=\frac{(C_0-C)\cdot G\cdot\rho_p}{m_p}\times 2.45 \tag{3}$$

where $C_0$ and $C$ are the initial and equilibrium concentrations of methylene blue solution, respectively. $G$ is the volume of methylene blue solution, and $m_p$ is the mass of the sample particles. The constant of 2.45 ($m^2$/mg of methylene blue) means that 1 mg of methylene blue could cover an area of 2.45 $m^2$ under the assumption of monomolecular-layer adsorption.

According to the cylindrical pore structural model, the mean pore diameter $D$ (nm) is estimated by

$$D=4\times 1000\times\frac{V_p(1-\omega)\rho_p}{S} \tag{4}$$

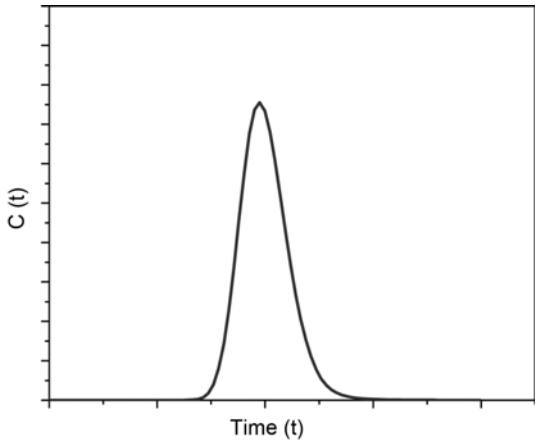


**Fig. 1.** Scheme of residence time distribution in packed bed. t is the normalized time and C(t) is the normalized concentration.

### 2.4. Mass transfer characteristics of MMAPs and MAPs

The mass transfer characteristics of MMAPs and MAPs were evaluated by measuring the retention time distribution (RTD) of different solutes (acetone, lysozyme, BSA, and IgG). The experiment was carried out with ÄKTA explorer 100 systems and C10/10 column (GE Healthcare, Uppsala, Sweden) packed with 5 mL magnetic particles. The flow rate was 1 mL/min. The chromatographic run was monitored on-line at 280 nm.

The typical curve of RTD is shown in Fig. 1, RTD could be described using the probability density function [14]. Assuming $m_k$ is the multi-order distribution of RTD, thus to the following expression:

$$\begin{cases} m_0 = A = \int_0^\infty C(t)dt \approx \sum_t C(t)\cdot\Delta t \\ m_1 = A = \int_0^\infty t\cdot C(t)dt \approx \sum_t C(t)\cdot\Delta t \\ \quad\cdots\cdots \\ m_k = A = \int_0^\infty t^k\cdot C(t)dt \approx \sum_t C(t)\cdot\Delta t \end{cases} \quad (5)$$

Assuming $\mu_k$ can be expressed as $\mu_k = \frac{m_k}{m_0}$, and then RTD time $\tau$ and $\sigma$ variance can be defined as follow,

$$\tau = \mu_1 = \frac{m_1}{m_0} \quad (6)$$

$$\sigma^2 = \mu_2^{\,2} - \mu_1^{\,2} \quad (7)$$

Assuming the dimensionless residence time $\theta = t/\tau$, and the dimensionless RTD $E(\theta)$ can be calculated by the following expression,

$$E(\theta) = C(t)\cdot\tau/m_0 \quad (8)$$

where $C(t)$ and $t$ can be measured through experiment.

### 2.5. Protein adsorption characteristics of MMAPs and MAPs

MMAPs and MAPs were modified with 5-amino-benzimidazol (ABI) named ABI- MMAPs and ABI-MAPs using the previous method [15,16] to evaluate the protein adsorption characteristics of MMAPs and MAPs. And the MMAPs without ABI ligand coupled were used as the control.

Typically, the magnetic particles were pre-equilibrated with sodium phosphate buffer (pH 7.0, 20 mM). Then, 1 mL IgG protein solution (0 ~ 10 mg/mL) was added into 2 mL tubes containing 0.04 g drained magnetic particles. The adsorption experiment was conducted at 25ºC for 3 h according to the adsorption kinetics experiment results (Fig. S1) in a thermo-mixer (1,500 rpm). At the end of adsorption, the particles were magnetically separated with the permanent magnet, and the protein concentration in the supernatant was determined at 280 nm with a spectrophotometer (OneDrop Technologies, Inc., LA, US). The adsorbed mass of protein was calculated according to mass balance. The Langmuir equation was employed to fit the experimental data as follow,

$$Q^* = \frac{Q_m C^*}{K_d + C^*} \quad (9)$$

where $Q^*$ is the equilibrium adsorption capacity (mg/mL), $C^*$ is the equilibrium protein concentration in the liquid phase (mg/mL), $Q_m$ is the maximum binding capacity (mg/mL) and $K_d$ represents the apparent dissociation constant (mg/mL).

### 2.6. Recycled use of MMAPs

The protein adsorption process was conducted as mentioned above, where the protein concentration of 3.5 mg/mL was used. After separated by permanent magnet, ABI-MMAPs were regenerated with 1.0 M NaOH and used for adsorption experiments again.

## 3. Results and Discussion

### 3.1. Morphology and size distribution of MMAPs

MMAPs were prepared by water-in-oil suspension method and the appearances of MMAPs were shown in Figs. 2 and 3. And the corresponding images for MAPs were shown in

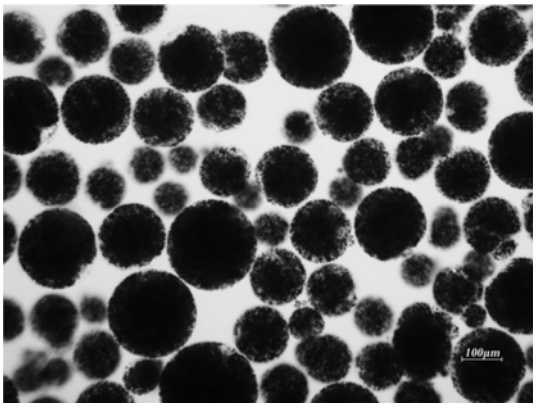


**Fig. 2.** Photograph of MMAPs appearance under the optical microscope (100×).

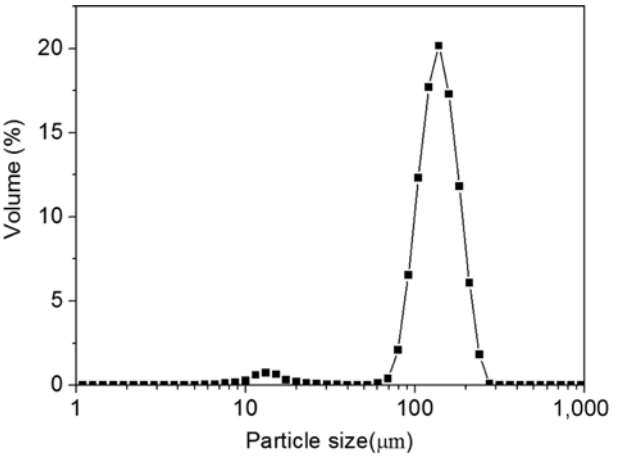


**Fig. 4.** Particle-size distributions of MMAPs.

Figs. S2 and S3. As seen from the optical microscope image, good sphericity was found and the crack of particles was hardly observed during the preparation for both MMAPs and MAPs. Moreover, the distribution of $Fe_3O_4$ embedded in the particles was relatively even. The fine morphology was examined by SEM. It could be found that macropores distributed densely and irregularly on the surface of MMAPs (Fig. 3), which were suspected to be beneficial for the protein transferring into the inner structure of the particles.

The particle-size distributions of MMAPs and MAPs were shown in Figs. 4 and S4, respectively. It was seen that the particle size showed a logarithmic symmetrical distribution with mean diameter of 127 μm for MMAPs and 154 μm for MAPs. About 80% of the MMAPs were in the range of 86 ~ 178 μm, hence the size distribution of MMAPs obtained was satisfying.

### 3.2. Physical properties of MMAPs

The physical properties of MMAPs including wet density ($\rho_p$), water content ($\omega$), porosity ($P$), pore volume ($V$), specific surface area ($S$), and mean pore diameter ($D$) were determined. Moreover, as a control, the normal magnetic agarose particles (MAPs) in the absence of calcium carbonate were also prepared by the same procedure.

As seen in Table 1, the wet density of MMAPs was almost the same as that of MAPs, while water content ($\omega$) of MMAPs was much higher than that of MAPs, indicating that the pore volume of particles was improved due to

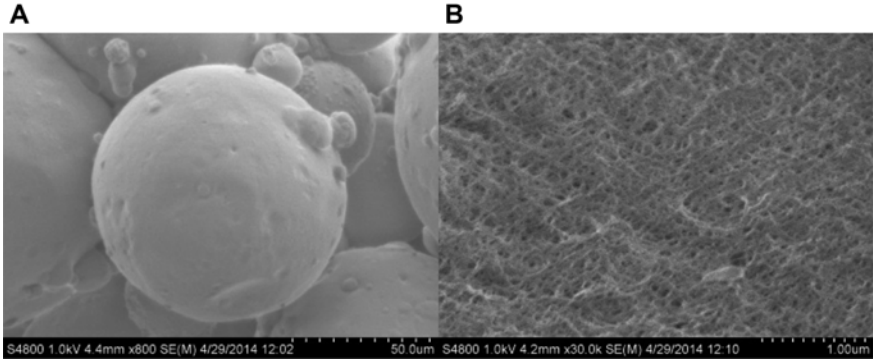


**Fig. 3**. Morphology of MMAPs by SEM. (A) the whole particle appearance of MMAPs; (B) surface structure of MMAPs.

**Table 1.** Physical properties of magnetic particles

| Adsorbent | $\rho_p$ (g/mL) | $\omega$ (%) | $P$ (%) | $V$ (mL/g) | $S$ ($m^2$/mL) | $D_p$ (nm) |
|---|---|---|---|---|---|---|
| MAPs | 1.04 ± 0.02 | 86.9 ± 2.1 | 90.7 ± 1.1 | 6.65 ± 0.12 | 67.4 ± 0.6 | 53.9 ± 3.5 |
| MMAPs | 1.02 ± 0.01 | 92.1 ± 3.0 | 94.4 ± 3.2 | 11.7 ± 0.15 | 31.4 ± 0.4 | 120.1 ± 8.3 |

MAPs: normal magnetic particles.
MMAPs: macroporous magnetic particles with calcium carbonate as the porogenic agent.

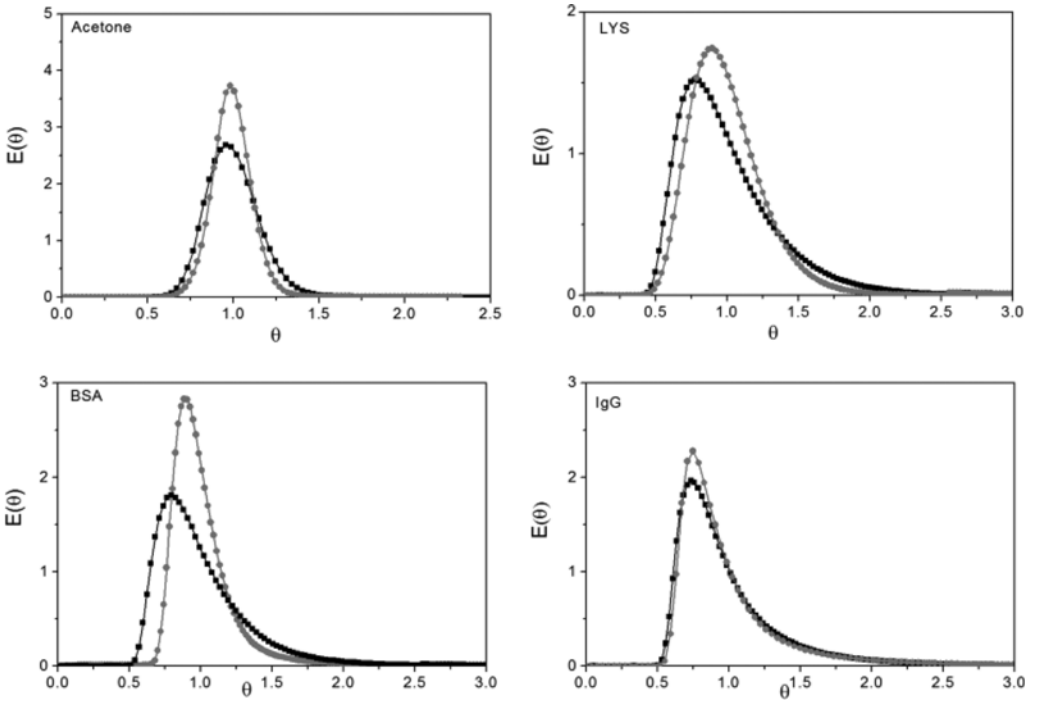


**Fig. 5.** Pore distribution comparison of MAPs and MMAPs by residence time distribution analysis. (■) MAPs, (●) MMAPs.

calcium carbonate addition during preparation. The porosity ($P$) means the pore volume per wet bead volume, reflecting the content of pore space in the beads. It could be seen that the porosity of the beads increased slightly with the addition of calcium carbonate, from 90.7 to 94.4%, suggesting the total pore volume was increased. The specific surface area ($S$) of MMAPs (31.4 ± 0.4 $m^2$/mL) was much lower than that of MAPs (67.4 ± 0.6 $m^2$/mL), which might be due to that the addition of pore forming agent enlarges the pore diameter but reduces the amount of micropores. The mean pore diameter increased significantly from 53.9 ± 3.5 to 120.1 ± 8.3 nm after calcium carbonate addition, correspondingly about 122% increase, confirming the successful generation of macropores .

### 3.3. Mass transfer characteristic of MMAPs

The experiments of RTD were carried out to study the mass transfer characteristic of MMAPs and MAPs. Acetone (58 Da), lysozyme (14 kD), BSA (66 kD), and IgG (150 kD) were adopted as the target molecules. The normalized RTD functions $E(\theta)$ as a function of normalized time $\theta$ for the MAPs and MMAPs were shown in Fig. 5. For both particles, the symmetry of elution peak became worse with tailing as the increase of the target molecule size, mainly arisen from the increased mass transfer resistance. However, compared with the MAPs, the symmetry of elution peak for MMAPs was much better and the elution peaks were higher and sharper. The above results clearly demonstrated that for MMAPs the mass transfer resistance was reduced to some extent, which might partially resulted from the presence of macropores inside the MMAPs. Besides, during the release process of carbon dioxide, carbon dioxide might breach the walls between the pores, leading to interconnection of the macropores. As a result, more channels were available and more pores in the agarose became accessible for protein transport, which also accounted for the reduced mass diffusion resistance of MMAPs. Such phenomena were also reported by Lu *et al.* [16]. In their work, the mass transportation performance was efficiently enhanced with the increase of pore size for MMI-coupled agarose matrices.

### 3.4. Protein adsorption of MMAPs

Finally, to evaluate whether the presence of macropores would affect the static protein adsorption performance of MMAPs, MMAPs were modified with the functional ligand ABI named ABI-MMAPs and the protein adsorption isotherm was measured with batch adsorption experiment. MAPs were also modified with ABI named ABI-MAPs for comparison. In addition, the MMAPs without ligand were also used. IgG was adopted as the model protein. The Langmuir equation was used to fit the experimental data. As shown in Fig. 6, the protein adsorption capacity of MMAPs without ligand was less than 12 mg/mL, indicating

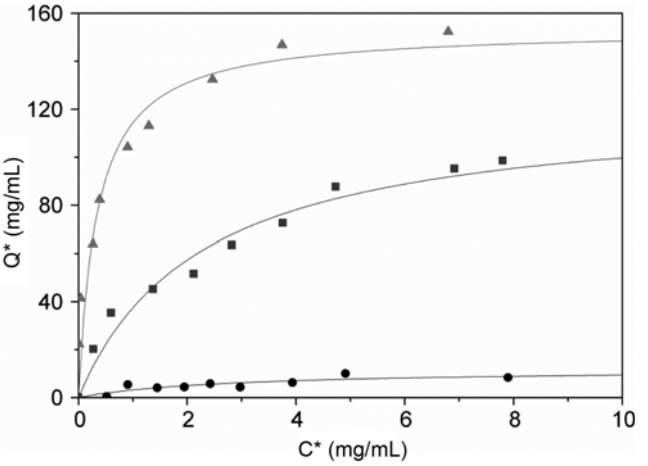


**Fig. 6.** The comparison of IgG adsorption with ABI-MMAPs, ABI-MAPs or MMAPs, respectively. Symbols represent experimental data, and solid lines represent the correlated results with Langmuir equation. (■) ABI-MAPs; (▲) ABI-MMAPs; (●) MMAPs.

the low non-specific adsorption. The adsorption capacity of IgG on ABI-MMAPs was higher than the corresponding value on ABI-MAPs during the IgG concentrations tested. The maximum adsorption capacity (153 mg/mL) of ABI-MMAPs was about 21% higher than that for ABI-MAPs (126 mg/mL), while the $K_d$ value for ABI-MMAPs (0.34 mg/mL) was much lower than that for ABI-MAPs (2.7 mg/mL), demonstrating the binding affinity of IgG with MMAPs was much higher. Other reported magnetic supports for protein adsorption showed a relatively low capacity [17-19].

The above phenomena were different from diethylaminoethyl (DEAE)-based superporous cellulose beads or agarose beads [11,12,20]. The reason might because that the adsorption capacity of absorbents was determined by various factors, such as properties of functional ligand, the efficient contacting area between the target proteins and the absorbent. In the present work, the agarose particles were modified with hydrophobic charge-induction chromatography ligand (ABI), so hydrophobic interaction which belongs to the physisorption dominated the binding process. Since hydrophobic interaction is a kind of short-range forces, presence of macropores would facilitate IgG in getting into the inner part of matrices and interacting with functional ligands.

### 3.5. Recycled use of MMAPs

To evaluate the stability of MMAPs, the particles were regenerated with 1 M NaOH after adsorption and recycled for BSA adsorption. As shown in Fig. 7, the adsorption capacity was little changed in twenty-five recycled adsorption, demonstrating the stability of MMAPs prepared herein as a magnetic adsorbent.

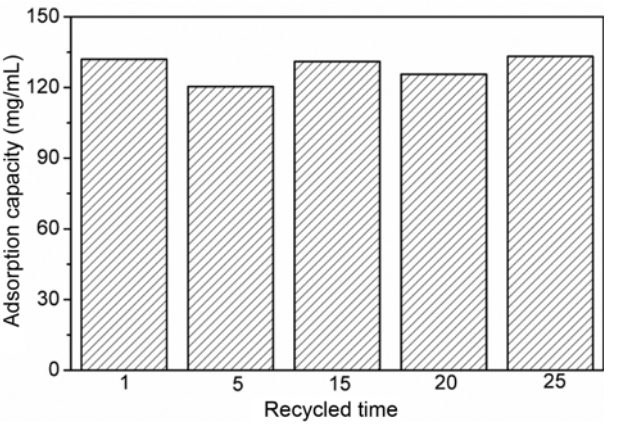


**Fig. 7.** Recycled use of ABI-MMAPs.

## 4. Conclusion

In the present work, MMAPs were prepared using calcium carbonate as the porogenic reagent through the method of water-in-oil suspension thermal regeneration. Compared with MAPs, physical properties for MMAPs including water content, porosity and mean pore size were significantly improved. Moreover, MMAPs exhibited higher protein adsorption capacity and reduced mass transfer resistance. The results demonstrated that MMAPs had superior characteristics as a potential medium for high-efficiency protein separation.

## Acknowledgements

This work was supported by Zhejiang Province Natural Science Foundation of China (Grant No. LQ16B060003), Scientific Research Fund of Zhejiang Province Education Department (Grant No. Y201533400), Natural Science Foundation of Huzhou (Grant No. 2015YZ05), Scientific Research Fund of Huzhou University (Grant No. 2015XJLK41).

## References

1. Chen, J., Y. Lin, and L. Jia (2015) Preparation of anionic polyelectrolyte modified magnetic nanoparticles for rapid and efficient separation of lysozyme from egg white. *J. Chromatogr. A* 1388: 43-51.
2. Zhou, L., Y. Shao, J. Liu, Z. Ye, H. Zhang, J. Ma, Y. Jia, W. Gao, and Y. Li (2014) Preparation and characterization of magnetic porous carbon microspheres for removal of methylene blue by a heterogeneous fenton reaction. *ACS Appl. Mater. Inter.* 6: 7275-7285.
3. Santana, S. D., V. L. Dhadge, and A. C. Roque (2012) Dextran-coated magnetic supports modified with a biomimetic ligand for

IgG purification. *ACS Appl. Mater. Interfaces* 4: 5907-5914.
4. Lin, Z., J. Zheng, Z. Xia, H. Yang, L. Zhang, and G. Chen (2012) One-pot synthesis of phenylboronic acid-functionalized core-shell magnetic nanoparticles for selective enrichment of glycoproteins. *RSC Adv.* 2: 5062-5065.
5. Zhao, M., Y. Xie, C. Deng, and X. Zhang (2014) Recent advances in the application of core-shell structured magnetic materials for the separation and enrichment of proteins and peptides. *J. Chromatogr. A* 1357: 182-193.
6. Li, D., Y. Zhang, M. Yu, Q. An, J. Guo, J.Q. Lu, and C. Wang (2015) A new strategy for synthesis of porous magnetic supraparticles with excellent biodegradability. *Chem. Commun.* 51: 1908-1910.
7. Nazari. S. F., P. Hashemi, and F. Rasoolzadeh (2015) A simple method for the preparation of spherical core-shell nanomagnetic agarose particles. *Colloid Surf. A Physicochem. Eng. Asp.* 465: 47-53.
8. Fujioka, H., M. Tsunehiro, M. Kawaguchi, Y. Kuramoto, H. Kurosaki, Y. Hieda, E. Kinoshita-Kikuta, E. Kinoshita, and T. Koike (2014) Simple enrichment of thiol-containing biomolecules by using zinc(II)-cyclen-functionalized magnetic beads. *J. Sep. Sci.* 37: 1601-1609.
9. Johnson, E. M., D. A. Berk, R. K. Jain, and W. M. Deen (1995) Diffusion and partitioning of proteins in charged agarose gels. *Biophys. J.* 68: 1561-1568.
10. Johnson, E. M., D. A. Berk, R. K. Jain, and W. M. Deen (1996) Hindered diffusion in agarose gels: Test of effective medium model. *Biophys. J.* 70: 1017-1023.
11. Shi, Q. H., X. Zhou, and Y. Sun (2005) A novel superporous agarose medium for high-speed protein chromatography. *Biotechnol. Bioeng.* 92: 643-651.
12. Du, K. F., S. Bai, X. Y. Dong, and Y. Sun (2010) Fabrication of superporous agarose beads for protein adsorption: Effect of $CaCO_3$ granules content. *J. Chromatogr. A* 1217: 5808-5816.
13. Xia, H. F., D. Q. Lin, and S. J. Yao (2007) Preparation and characterization of macroporous cellulose-tungsten carbide composite beads for expanded bed applications. *J. Chromatogr. A* 1175: 55-62.
14. Levenspiel, O. (1999) *Chemical Reaction Engineering*. 3rd Ed., pp. 257-277. John Wiley and Sons (WIE), NY, USA.
15. Gao, D., S. J. Yao, and D. Q. Lin (2008) Preparation and adsorption behavior of a cellulose-based, mixed-mode adsorbent with a benzylamine ligand for expanded bed applications. *J. Appl. Polym. Sci.* 107: 674-682.
16. Lu, H. L., D. Q. Lin, D. Gao, and S. J. Yao (2013) Evaluation of immunoglobulin adsorption on the hydrophobic charge-induction resins with different ligand densities and pore sizes. *J. Chromatogr. A* 1278: 61-68.
17. Tong, X. D., B. Xue, and Y. Sun (2001) A novel magnetic affinity support for protein adsorption and purification, *Biotechnol. Progr.* 17:134-139.
18. Tong, X. D. and Y. Sun (2001) Agar-based magnetic affinity support for protein adsorption. *Biotechnol. Progr.*17:738-743.
19. Liu, X. Y., S. W. Zheng, R. Y. Hong, Y. Q. Wang, and W. G. Feng (2014) Preparation of magnetic poly(styrene-co-acrylic acid) microspheres with adsorption of protein. *Colloid Surf. A Physicochem. Eng. Asp.* 443:425-431.
20. Wang, D. M., G. Hao, Q. H. Shi, and Y. Sun (2007) Fabrication and characterization of superporous cellulose bead for high-speed protein chromatography. *J. Chromatogr. A* 1146: 32-40.